Effect of Groove Designs on Residual Stress and Transverse Shrinkage in GMAW and PGMAW of A333 Seamless Steel Pipes

Rohit Mishra[*,§], Avani Kumar Upadhyay[†,¶], Amneesh Singla[†,‖] and Yashvir Singh[‡,**]

[*]*Department of Mechanical Engineering*
Jaypee University of Engineering and Technology
Guna, M. P., India

[†]*Department of Mechanical Engineering*
University of Petroleum and Energy Studies
Dehradun, U. P., India

[‡]*Department of Mechanical Engineering*
Graphic Era Deemed to be University
Dehradun, Uttarakhand, India
[§]*rohitmishra2288@gmail.com*
[¶]*akupadhyay@ddn.upes.ac.in, avani.mech@gmail.com*
[‖]*amneesh82@gmail.com, asingla@ddn.upes.ac.in*
[**]*yashvirsingh21@gmail.com*

The effectiveness of weld joints primarily depends on the fusion of base metal, minimum heat-affected zone (HAZ) and lesser residual stresses. The severity of thermomechanical effects e.g. weld shrinkages and residual stresses is significantly minimized by narrow gap welding technique over the traditional welding. This work describes the welding of A333 Grade 3 steel pipes by the application of GMAW and PGMAW techniques. The analysis is made to capture the effects of groove designs on residual stress and transverse shrinkage. The process parameters used for the analysis are voltage, current and welding speed. In this work, narrow groove design using PGMAW process is capable of reducing the number of passes and area of weld deposit by 35–40% by volume. In PGMAW, decrement in residual stresses is observed with a narrow groove compared to conventional V groove technique. The results are validated by metallurgical and mechanical investigation of welded joints. This work will help other researchers to understand the effect of narrow gap welding using an optimum number of passes for thick pipes.

Keywords: Transverse shrinkage; PGMAW; residual stresses; HAZ; narrow groove design; A333 steel.

1. Introduction

Mild steel pipes of various thickness are accessible financially and have a wide scope of utilization in the development of cutting edge structures. Mechanical properties of these steels mainly depend on the chemical composition of the constituents. A333,

*Corresponding author.

Grade 3 pipes have great formability and weldability. These alloys have high yield strength and ultimate tensile strength, i.e. 240 and 450 MPa, respectively. According to American piping products , A333 steel pipe is good for low-temperature applications.[1]

Welding is majorly used in the construction and piping industries. Welded joints are subjected to severe residual distortion because of weld thermal cycles.[2–4] The residual stresses cause many problems such as crack, performance deterioration, shrinkage and less strength.[5] Therefore, it is necessary to measure the shrinkage and associated residual stress produced during the welding.[6] Moreover, there is a requirement to develop a suitable welding technique for minimizing residual stresses in the weld.

Common processes for thick pipe welding are SMA, FSW, TIGW and gas metal arc welding (GMAW). These processes influence the weld thermal cycle, amount of weld deposition, shielding environment and the various welding parameters.[7–9] PGMAW process was first used in late 80s and has better control on the arc for sound welds.[10,11] Better control on the arc in GMAW process is due to peak current (I_p), base current (I_b), frequency (f), peak pulse duration (t_p), base current duration (t_b), etc. These parameters provide comparatively low heat input. A dimensionless key factor $Ø = [(I_b/I_p)f^*t_b]$ is used to influence the pulse characteristics.[9,12–14]

Large thermal gradients can be developed in the welding of the thicker section due to uneven localized heating and cooling cycle in the weld region. A significant misfit strain will be developed due to the difference in the expansion and contraction of the material being welded. Diffident value of the misfit can be attuned by elastic strain. However, very high misfit strain induces localized plastic deformation resulting in the development of residual stresses. When the component comes under thermal equilibrium, noteworthy residual stresses occur near the weld. This case can be found predominantly for the thicker sections due to a large number of thermomechanical cycles.[15] For large components, it is difficult to apply the residual stress removal techniques like shot peening, laser shock peening, etc.[16]

In a heavy plate, GMAW with narrow groove design provides maximum efficiency and better quality as compared to traditional welding.[17] The severity of thermomechanical effects can be significantly reduced by lowering the volume of weld metal in a joint and the same can be achieved by a narrow gap welding technique for thicker sections. Narrow groove also provides better productivity due to less weld volume and lesser welding time. Tan *et al.*. demonstrated the narrow gap TIG welding of nuclear rotor steel pipes. They studied the residual stress developed using the hole drilling technique.[18] Xu *et al.* studied the mechanical and microstructural properties of HSLA steel fabricated by narrow gap welding. Efforts have not been done to compare the residual stresses generated in varied groove designs. This work is being carried out to evaluate the residual stress and transverse shrinkage (TS) using GMAW and PGMAW process. For better results, a comparison of these processes with narrow groove design has been reported.

2. Materials and Methods

2.1. *Base material*

The investigation has been carried out using 22 mm thick and 230 mm outer diameter A333 Grade 3 pipe. The composition of the base material has been examined by optical emission 0spectroscopy (Spectromax Lmf_01) in the laboratory. Table 1 shows the elemental composition of the base metal.

2.2. *Welding consumable*

Continuous current GMAW and PGMAW processes were carried out with the copper-coated continuous solid-state electrode WAS/SFR 5.18 ER: 70S-6 (Raajratna electrode private ltd.) in an inert environment. The gas contains the composition of 80% argon and 20% CO_2. The composition of filler metal used in the welding process is mentioned in Table 2.

2.3. *Groove design*

Welding was done by two different techniques that include GMAW with a continuous current and pulsed current. Welding, which was performed on different groove designs, is shown in Fig. 1.

2.4. *Welding setup*

A modern transistorized power source of ESAB (ARISTO 2000-LUD 450 UW) was used for welding. In the power source, peak current (I_P) and base current (I_b) were capable to operate in the steps of 4A, whereas the pulse frequency and peak duration in the steps of 2 Hz and 0.1 ms, respectively.A suitable fixture for welding of pipes in 1-GR position is shown in Fig. 2. The welding system has a manipulator for controlling the rotation of the pipe. A flexible torch holding and positioning facility

Table 1. Elemental composition of base metal.

Material (A333 Grade 3)	Source	Chemical analysis (weight%)								
		C	Si	Mn	p	S	Cr	Ni	Al	Cu
	*Laboratory test	0.2047	0.1964	0.5981	0.0122	0.0070	0.0635	0.1668	0.0392	0.018

Table 2. Chemical composition of filler metal.

Filler metal	Composition (weight%)					
	C	Mn	Si	S	P	Cu
	0.15	1.40	0.80	0.035	0.025	0.50

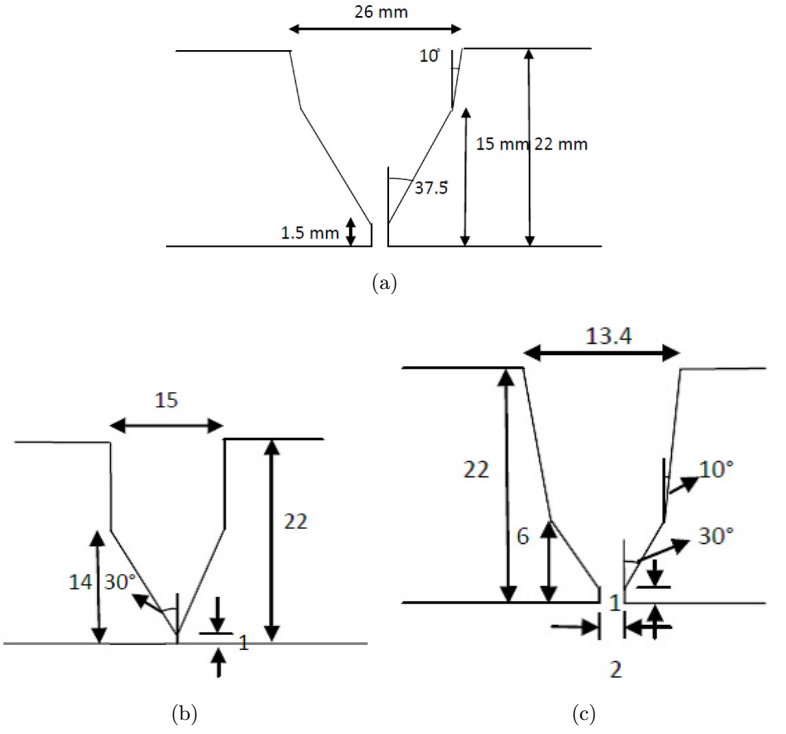

Fig. 1. Schematic images (a) conventional groove 26 mm main opening, (b) narrow groove 15 mm main opening and (c) narrow groove 13.4 mm main opening.

fitted with modern torch carriage trolley for GMAW and PGMAW pipe welding support this manipulator. The welding speed for a given dimension of pipe can be controlled in the range of 1.0–19 cm/min by an electronically controlled mechanism (AC drive).

The welding setup consists of an automated GMAW gun, traveling equipment and a travel carriage trolley. For the desired position adjustment, clamping pivots are fitted to the setup. The traveling equipment with a digital display is used to record traveling speed with a range of 2.6–83.8 cm/min. The torch carriage trolley also supports the positioning of the torch during welding. The manipulator has a three-jaw chuck for firm holding and centering of pipes.

2.5. *Welding procedure*

The welding was carried out in two steps, i.e. root pass and filler pass. Root pass weld was performed in an inert environment (commercial argon) using a tungsten electrode of 3.2 mm in diameter. The torch used for this welding was water-cooled and equipped with a gas nozzle of diameter 7 mm. Filler pass was performed using GMAW on conventional groove and PGMAW on mentioned narrow grooves in 1-GR position. Tables 3 and 4 show the parameters for root pass and filler pass

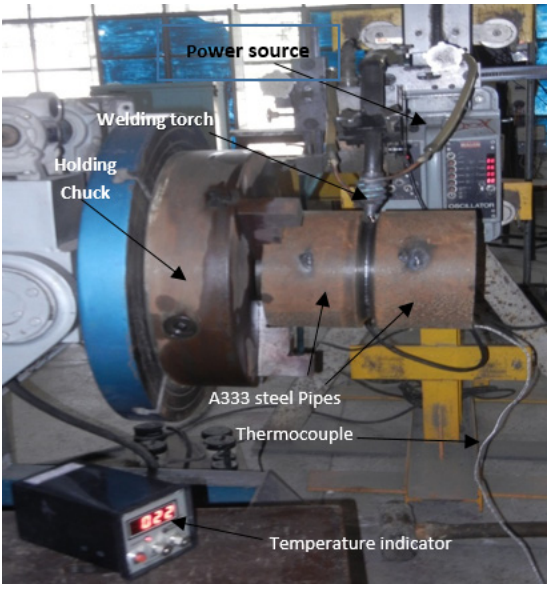

Fig. 2. Photograph showing pipe-holding fixture, thermocouple and torch manipulator used in welding of pipes.

Table 3. The parameter used for root pass.

Voltage (V)	Current (A)	Welding speed (cm/min)
12	110	6–7

Table 4. Welding parameters

Welding process	Voltage (V)	Heat input	Travel speed (cm/min)	I/I_m (A)	Pulse parameters				
					I_p (A)	I_b (A)	f (Hz)	t_b (ms)	t_p (ms)
GMAW	24 ± 1	11.6 ± 0.5	20	230 ± 4	—	—	—	—	—
P-GMAW	24 ± 1	9.5 ± 0.5	16	160	324	160	50	13	7

welding, respectively. The gas flow rate used during the welding process was 12 L/min for all cases.

2.6. *Measurement of residual stresses*

The residual stresses at the top and root of the pipe weld were measured by placing a three-element strain gauge rosette system (HMB RY1) at desired locations and using the hole drilling technique. The measurement of residual stresses has been carried out at different locations such as a weld, heat-affected zone (HAZ), fusion line (FL), etc.

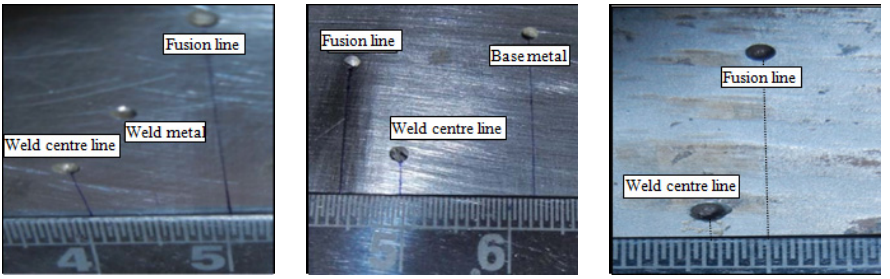

(a) (b) (c)

Fig. 3. Location of the drill after residual stress measurement at (a) top in conventional groove, (b) top in a narrow groove and (c) root of the weld joint.

The surface of selected regions for the measurement of residual stresses was mechanically smoothened and cleaned by acetone prior to fixing the strain gauge. Locations of a drill made during residual stress measurement for different groove designs are shown in Fig. 3.

2.7. *Measurement of Transverse shrinkage*

TS investigation was done with a simple line drawing method. Parallel Lines were drawn across weld at four different circumferential locations, as shown in Fig. 4. They had been punch-marked before welding. Cumulative difference in the length of the lines was measured after each pass of the welding. The test had been carried out for GMAW and PGMAW with the defined groove designs.

2.8. *Estimation of shrinkage stresses*

TS stress ($\sigma_{trs(i-j)}$) is a function of heat supplied and thickness of pipe.[19,20] Calculations of TS stress under varied thermal behavior are as follows[21]:

$$\sigma_{\mathrm{trs}(i-j)} = \frac{\Delta_{\mathrm{trs}}}{N} \times \frac{a_{\mathrm{th}}}{t} \times \frac{E}{L_{\mathrm{st}}}, \tag{1}$$

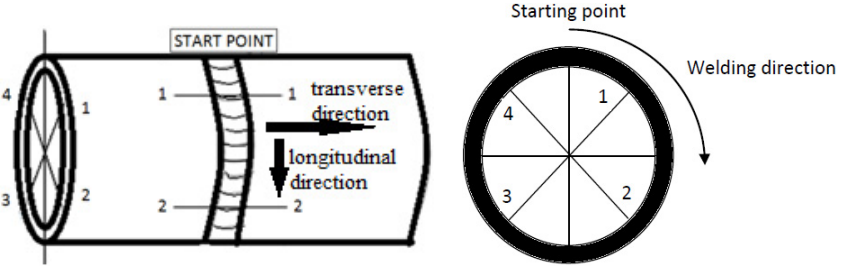

Fig. 4. Schematic images of the weld showing circumferential locations for measurement of shrinkage stresses.

where

(Δ_{trs}) = Measured TS (mm),

N is the number of deposited weld coats,

E is Young's Modulus of elasticity (240 GPa),

L_{st} is the straining size,

t is the pipe thickness,

a_{th} is the average height of weld deposited per coat and

Standard deviation (SD) is calculated with the help of average TS stress, as shown in Eq. (4).

$$\sigma_{(i-j)} = \frac{\sigma_{i-i} + \sigma_{j-j}}{2}, \tag{2}$$

$$\sigma_a = \sum_{i=0}^{4} \frac{\sigma_{\text{trs}(i-j)}}{4} \tag{3}$$

$$\text{SD} = \sqrt{\left(\frac{1}{4} \times \sum_{i=0}^{4} (\sigma_{(i-j)} - \sigma_a)^2\right)}. \tag{4}$$

Based on the above procedure, transverse stress at various positions of pipe weld has been estimated.

3. Results and Discussion

3.1. *Transverse shrinkage*

Cumulative TS at numerous locations for A333 pipe welds for conventional and narrow grooves are shown in Table 5. The approximation of $\sigma_{\text{trs}(i-i)}$, σ_a and SD for straining size of 80 and 75 mm for conventional and narrow grooves, respectively, are shown in Table 6. TS stresses $\sigma_{\text{trs}(i-j)}$ and their nature for different samples are given in Tables 8–11. Large variation is observed in the shrinkage stresses. Tables 7 and 8 show the shrinkage stresses and their nature at different locations of the pipe weld. Mixed tensile and compressive nature are observed at different locations. Tables 9 and 10 show the nature of shrinkage stresses in the case of narrow groove welding. A significant decrease in the shrinkage stresses can be seen as compared to conventional

Table 5. TS at different positions of A333 pipe welds.

Sample	Weld	Heat input (KJ/cm)	Cumulative shrinkage (Δ_{trs}) at different locations on pipe (mm)				Average shrinkage (mm)
			1-1	2-2	3-3	4-4	
1	PGMAW	9.5	1.52	1.41	1.45	1.14	1.36
2	GMAW	11.6	2.54	2.01	2.95	2.05	2.07
3	PGMAW (15 mm)	9.5	1.46	1.22	0.89	1.03	1.15
4	PGMAW (13.4 mm)	9.5	1.14	1.10	1.11	1.12	1.06

Table 6. TS for conventional and narrow groove weld joints.

Sample	Weld	Heat supplied (KJ/cm)	Calculated TS stress at different locations (MPa)				Average TS stress ± SD
			1-1	2-2	3-3	4-4	
1	PGMAW	9.5	80.56	74.73	81.88	63.49	75.165 ± 2.8
2	GMAW	11.6	148.09	108.34	166.58	114.18	134.29 ± 4.73
3	PGMAW (15 mm)	9.5	109.63	93.16	71.20	81.2	88.6 ± 9.9
4	PGMAW (13.4 mm)	9.5	85.60	84.0	88.80	88.37	86.69 ± 1.35

Table 7. Nature of TS at various locations of conventional GMAW.

Weld location	TS stress (MPa)	Nature	Average TS stress ± SD
1-2	128.215	Compressive	134.29 ± 4.73
2-3	137.46	Tensile	
3-4	140.38	Tensile	
4-1	131.135	Compressive	

Table 8. Nature of TS at various location of conventional PGMAW.

Weld location	TS stress (MPa)	Nature	Avg. TS stress ± SD
1-2	77.645	Tensile	75.165± 2.8
2-3	78.305	Tensile	
3-4	72.685	Compressive	
4-1	72.025	Compressive	

Table 9. Nature of TS at various location of narrow PGMAW having groove width 15.

Weld location	TS stress (MPa)	Nature	Average TS stress ± SD
1-2	101	Tensile	88.6 ± 9.9
2-3	82.1	Compressive	
3-4	76.2	Compressive	
4-1	95.1	Tensile	

Table 10. Nature of TS at different location of narrow PGMAW having groove width 13.4.

Weld location	TS stress (MPa)	Nature	Average TS stress ± SD
1-2	84.8	Compressive	86.69 ± 1.35
2-3	86.4	Compressive	
3-4	88.585	Tensile	
4-1	86.985	Tensile	

welding and are well within the yield strength of the materials hence welds are safe and within the limits.

3.2. *Effect of multi-passes on shrinkage stresses*

The comparison of TS in all grooves after each pass is shown in Fig. 5(a). PGMAW process gives lesser heat input than GMAW process, therefore, TS is lesser in PGMAW. Moreover, in GMAW, the mode of metal transfer is generally globular which can be converted to spray transfer at higher current value (more than 190 Ampere), but in PGMAW, mode of metal transfer is pulsed therefore GMAW imparts higher weld deposition area as compared to PGMAW process. Due to the pulsed mode of current in PGMAW weld, the mean current value for PGMAW process is much less than conventional GMAW.[22] Parameters used for narrow groove welding are the same for both groove designs but the difference comes in their weld deposition area. The weld deposition area is higher in narrow groove 1 than narrow groove 2, as shown in Table 11. High metal deposition increases the shrinkage in narrow groove 1 than shrinkage in narrow groove 2. We can observe increment in TS with an increase in a number of passes as the material will be under the heating condition for larger time and subsequently the severity of weld thermal cycle increases. Lowest shrinkage is detected in 13.4 PGMAW with eight passes.

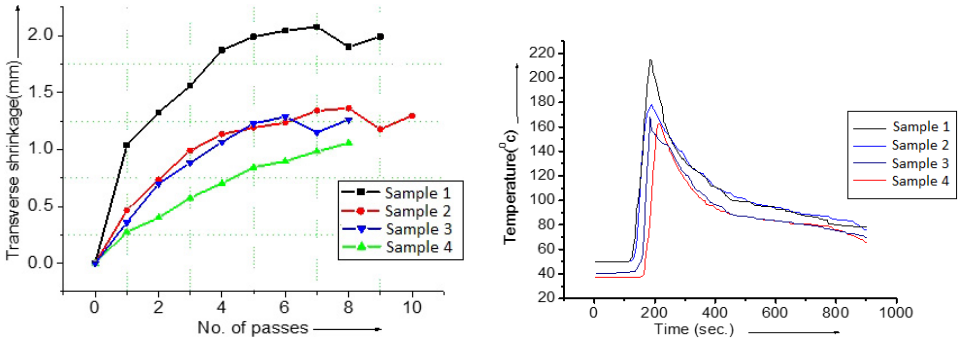

Fig. 5. (a) Cumulative shrinkage for all welds and (b) thermal profile for all welds.

Table 11. Groove area for conventional and narrow grooves.

Design of groove	Groove area (Sq.mm)
Conventional (groove width 26)	338.12
Narrow 1 (groove width 15)	217.50
Narrow 2 (groove width 13.4)	202.34

The thermal profile reveals the peak temperature and the maximum temperature is observed in the case of GMAW than that of PGMAW, as shown in Fig. 5(b).

3.3. *Residual stresses*

Figures 6(a)–6(d) show longitudinal and transverse stress distribution on inner and the outer surface for GMAW and PGMAW with conventional groove design. Results show that PGMAW process has 35–45% lesser longitudinal residual stress at top surface compared to the GMAW process. The lesser difference is three in the case of transverse residual stresses but is still around 15%. Similar types of results have been found at the bottom surface but with lesser magnitude. Figures 7(a)–7(d) show the value of longitudinal residual stresses for PGMAW with narrow grooves at the top and bottom surface. 13 mm groove is having around 12% lesser longitudinal stresses

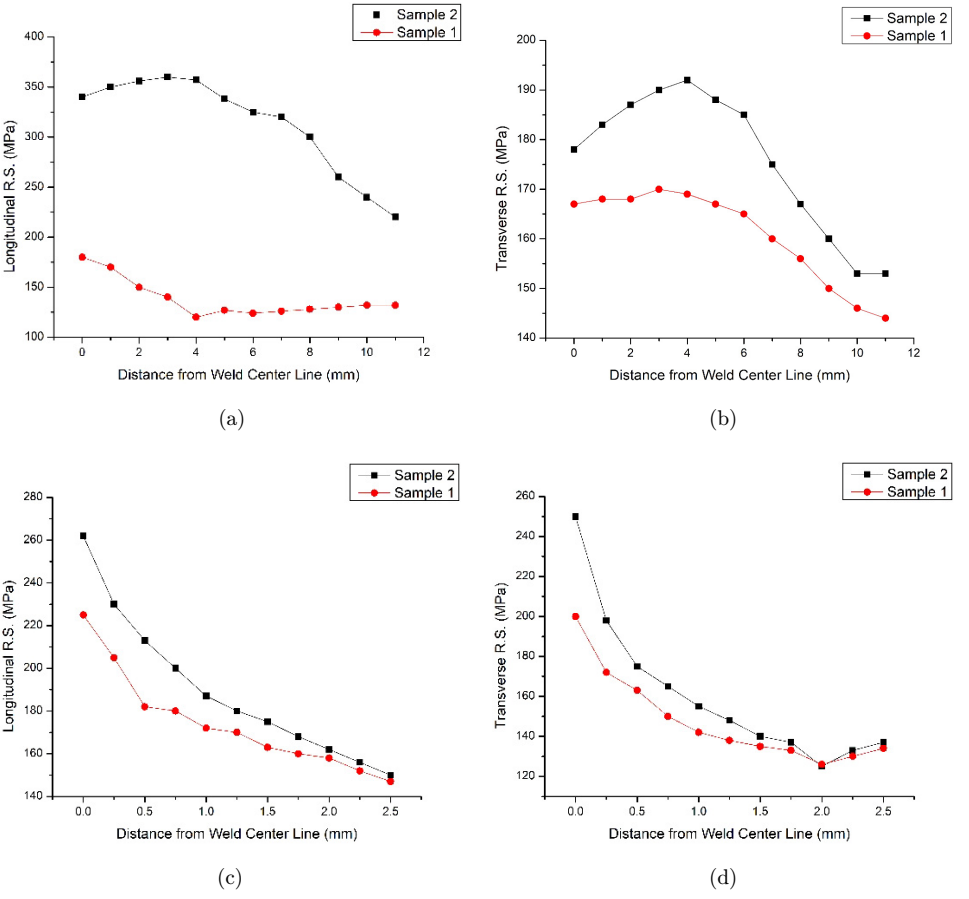

Fig. 6. Comparison of residual stress distribution for conventional groove GMAW and PGMAW. (a) Longitudinal stress distribution on top surface, (b) TS distribution on top surface, (c) longitudinal stress at bottom surface and (d) transverse stresses at bottom. surface.

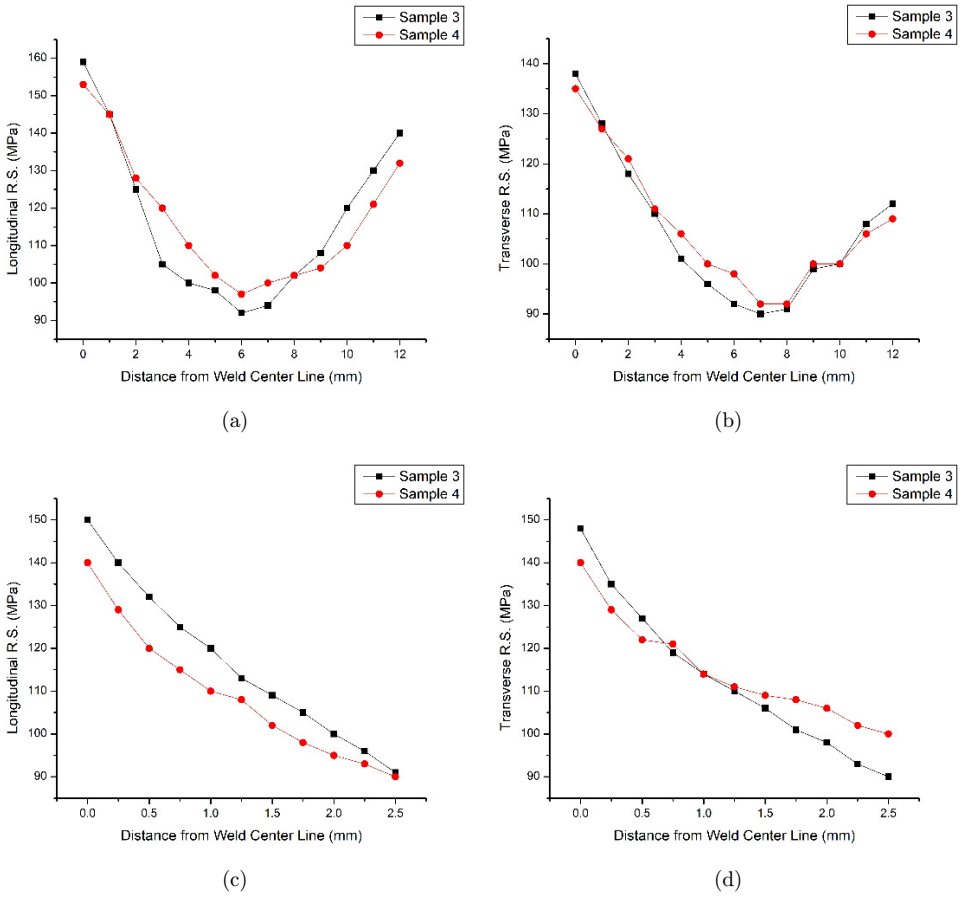

Fig. 7. Comparison of residual stress distribution for narrow groove GMAW PGMAW. (a) Longitudinal stress distribution on top surface, (b) TS distribution on top, (c) longitudinal stress at bottom and (d) transverse stresses at the bottom.

at the top and bottom surfaces, as compared to 15 mm groove. A considerable difference in the growth of residual stresses for conventional and narrow gap welds may be attributed primarily to the severity of thermomechanical characteristics. The severity arises due to differential expansion and contraction stresses during multi-pass deposition. In the case of narrow gap welding, the severity of thermomechanical characteristics decreases up to a certain extent due to the lesser amount of weld deposits and phase transformations.[22]

3.4. *Material characterization*

The microstructure of the base metal, weld+ HAZ and weld metal for conventional groove GMAW is shown in Fig. 8. Microstructure displays the conventional behavior of multi-pass welds comprises coaxial dendrites and reheat refined areas. Figure 9

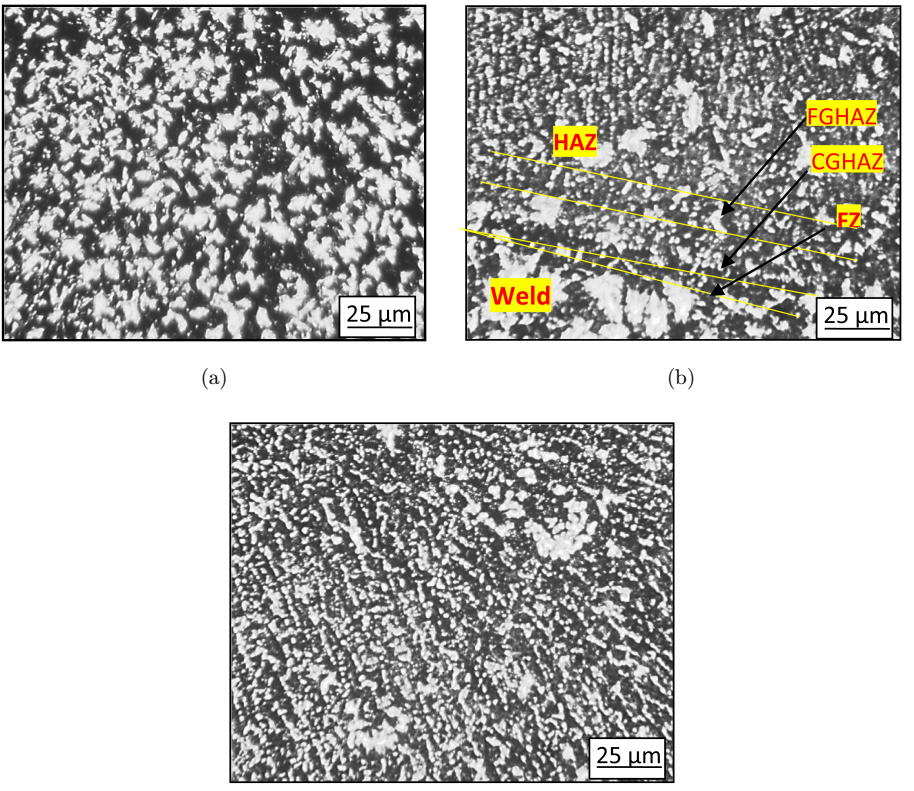

(a) (b)

(c)

Fig. 8. The microstructure of sample 2 (a) base metal; (b) Weld + HAZ and (c) Weld.

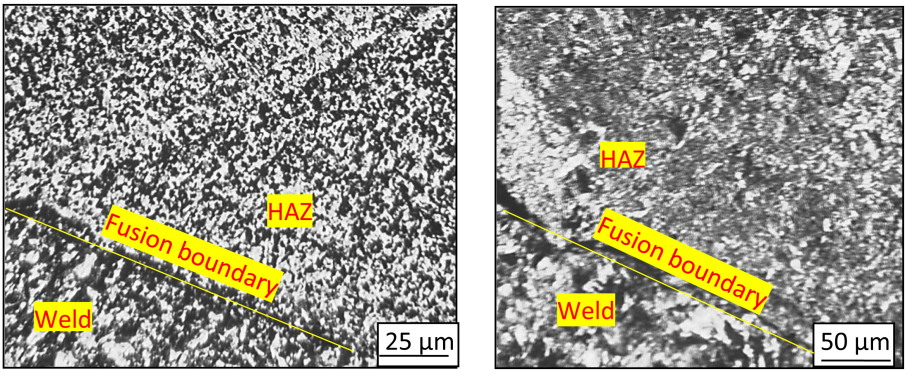

(a) (b)

Fig. 9. The microstructure of Weld + HAZ (a) sample 1, (b) sample 3 and (c) sample 4.

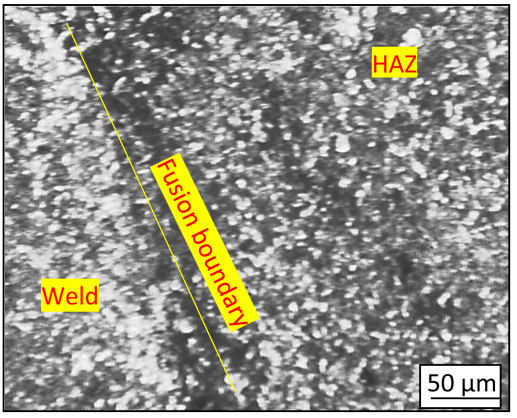

(c)

Fig. 9. (*Continued*)

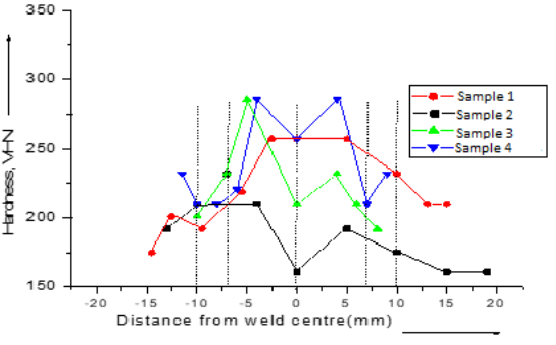

Fig. 10. Variation in hardness observed in welded joints.

shows the microstructure of PGMAW. We can observe considerable grain refinement with the scarcely distributed coaxial dendritic structure in case of PGMA welds and is in good agreement with previously reported work.[23] The microstructure consists of weld zone (WZ), fusion zone (FZ) having lath martensitic structure. Next to the FZ, there is coarse grain and fine grain HAZ (CGHAZ and FGHAZ). Conventional GMAW is having nearly 1 mm width of CGHAZ and 4 mm width of FGHAZ. The highest hardness of around 300 HV is observed in the CGHAZ, as shown in Fig. 10. Average grain size found in CGHAZ is around 250 μm in case of conventional groove whereas it is reduced to 180 μm in case of narrow grooves.

4. Conclusions

Estimation of TS stresses was carried out for different groove designs. Average shrinkage stress developed for GMAW and PGMAW using conventional groove had

been estimated as 134.29 and 75.16 MPa, respectively, whereas it was found to be around 88 MPa in case of narrow groove design with PGMAW. In comparison to conventional groove GMAW, PGMAW can produce sound welds at a comparatively lower heat input (9.5 + 0.3 kJ/cm). PGMAW reduces TS than that of GMAW.

(1) Shrinkage stresses were increasing with increment in a number of weld passes. PGMAW process using narrow groove design reduces the number of passes and area of weld deposit by 35–40%.
(2) Nature of shrinkage stresses is different at different locations of the pipe. This nature depends on the procedure of welding.
(3) Longitudinal and transverse residual stresses developed were tensile in nature. Their magnitude varies with respect to location, process and groove design. Narrow groove design was suitable because of the lesser value of longitudinal and transverse residual stresses. In PGMAW (conventional groove), longitudinal residual stress at the top surface was 35–45% lesser compared to GMAW. Maximum transverse residual stresses in conventional groove design at the top surface were 190 and 170 MPa in GMAW and PGMAW, respectively. Maximum longitudinal and transverse residual stresses in narrow groove design were 160 and 140 Mpa, respectively. Variation in the magnitude of residual stresses was lesser in the narrow groove than that of conventional V-groove design.
(4) PGMAW reduces coaxial dendrites by almost 10–15% than conventional groove welds.

References

1. W. H. Kearns, Brazing, in *Welding Handbook* (Macmillan Education, UK, 1978), pp. 369–438.
2. C. R. Taylor, Carbon dioxide-based refrigerant systems, *ASHRAE J.* **44**(9) (2002) 22.
3. S. Okano and M. Mochizuki, Transient distortion behavior during TIG welding of thin steel plate, *J. Mater. Process. Technol.* **241** (2017) 103–111.
4. S. Song and P. Dong, A framework for estimating residual stress profile in the seam-welded pipe and vessel components part I: Weld region, *Int. J. Press. Vessels Pip.* **146** (2016) 74–86.
5. M. N. James, Design, manufacture, and materials; their interaction and role in engineering failures, *Eng. Fail. Anal.* **12**(5) (2005) 662–678.
6. Z. Chen, Z. Chen and R. A. Shenoi, Influence of welding sequence on welding deformation and residual stress of a stiffened plate structure, *Ocean Eng.* **106** (2015) 271–280.
7. D. D. Deshmukh and V. D. Kalyankar, Deposition characteristics of multitrack overlay by plasma transferred arc welding on SS316L with Co-Cr based alloy–influence of process parameters, *High Temp. Mater. Process.* **38**(2019) (2019) 248–263.
8. W. Yang, J. Xin, C. Fang, W. Dai, J. Wei, J. Wu and Y. Song, Microstructure and mechanical properties of ultra-narrow gap laser weld joint of 100 mm-thick SUS304 steel plates, *J. Mater. Process. Technol.* **265** (2019) 130–137.
9. P. K. Ghosh, S. G. Kulkarni, M. Kumar and H. K. Dhiman, Pulsed current GMAW for superior weld quality of austenitic stainless steel sheet, *ISIJ Int.* **47**(1) (2007) 138–145.

10. M. Amin, Synergic control in MIG welding. I. Parametric relationships for steady DC open arc and short circuiting arc operation, *Met. Constr.* **19**(1) (1987) 22–28.
11. M. Amin, Pulse current parameters for arc stability and controlled metal transfer in arc welding, *Met. Constr.* **15**(5) (1983) 272–278.
12. P. K. Ghosh and L. Dorn. Thermal behavior of pulsed MIG AL-Zn-MG alloy welds-An analytical model, *Int. J. Joining Mater.* **5** (1993) 143.
13. P. K. Ghosh and P. C. Gupta, Use of pulse current MIG welding improves the weld characteristics of Al-Zn-Mg Alloy, *Indian Weld. J.* **29** (1996) 24–32.
14. P. Ghosh, P. Gupta and V. Goyal, Stainless steel cladding of structural using the pulsed current GMAW process, *Wield J. (Mami, Fla)* **77** (1998) 307-s.
15. V. K. Goyal, P. K. Ghosh and J. S. Saini, Process-controlled microstructure and cast morphology of dendrite in pulsed-current gas-metal arc weld deposits of aluminum and Al-Mg alloy, *Metall. Mater. Trans. A* **38**(8) (2007) 1794–1805.
16. M. Hu, K. Li, Z. Cai and J. Pan. A new weld material model used in welding analysis of narrow gap thick-walled welded rotor, *J. Manuf. Process.* **34** (2018) 614–624.
17. V. Y. Malin, The state-of-the-art of narrow gap welding part II, *Weld. J.* **62** (1983) 37–46.
18. J. Haidar and J. J. Lowke, Predictions of metal droplet formation in arc welding, *J. Phys. D, Appl. Phys.* **29**(12) (1996) 2951.
19. S. Kou. A simple index for predicting the susceptibility to solidification cracking, *Weld. J.* **94** (2015) 374s–388s.
20. V. N. Panin, Experimental-calculation estimation of residual welding distortions in shells of turbine penstocks at hydraulic power stations, *Paton Weld. J. C/C Avtomaticheskaia Svarka* **2007**(5) (2007) 7.
21. N. Jacobsen. Monopulse investigation of drop detachment in pulsed gas metal arc welding, *J. Phys. D, Appl. Phys.* **25**(5) (1992) 783.
22. P. K. Ghosh, L. Dorn, M. Hübner and V. K. Goyal, Arc characteristics and behavior of metal transfer in pulsed current GMA welding of aluminum alloy, *J. Mater. Process. Technol.* **194**(1–3) (2007) 163–175.
23. R. Wu and F. Seitisleam. Influence of extra coarse grains on the creep properties of 9 percent CrMoV (P91) steel weldment, *J. Eng. Mater. Technol.* **126**(1) (2004) 87–94.